

QUANTIFYING THE EFFECT OF COSMIC RAY SHOWERS ON THE X-IFU ENERGY RESOLUTION

Peille, P.¹; den Hartog, R.²; Miniussi, A.³; Stever, S.⁴; Bandler, S.³; Kirsch, C.⁵; Lorenz, M.⁵; Dauser, T.⁵; Wilms, J.⁵; Lotti, S.⁶; Gatti, F.⁶; Macculli, C.⁶; Jackson, B.²; Pajot, F.⁷

¹CNES, France; ²SRON, The Netherlands; ³GSFC, USA; ⁴IPMU, Japan; ⁵Remis Observatory & ECAP, Germany; ⁶INAF, Italy; ⁷IRAP, France

Abstract: The X-ray Integral Field Unit (X-IFU) will operate an array of more than 3000 Transition-Edge Sensor pixels at 90 mK with an unprecedented energy resolution of 2.5 eV at 7 keV. In space, primary cosmic rays and secondary particles produced in the instrument structure will continuously deposit energy on the detector wafer and induce fluctuations on the pixels' thermal bath. We have investigated by simulation of the X-IFU readout chain how these fluctuations eventually influence the energy measurement of the science photons. Realistic timelines of thermal bath fluctuations at different positions in the array are generated as a result of a thermal model and the expected distribution of the deposited energy of the charged particles. These are then used to model the TES response to these thermal perturbations and their influence on the on-board energy reconstruction process. Overall, we show that with adequate heatsinking, the main energy resolution degradation effect remains minimal and within the associated resolution allocation of 0.2 eV. We further study how a dedicated triggering algorithm could be put in place to flag out the rarer large thermal events.

COSMIC RAY ENVIRONMENT

Cosmic rays present at the future X-ray Integral Field Unit [1] L2 orbit (mostly protons) will interact with the instrument structure and induce energy depositions in...

► ... the X-IFU pixels creating fake X-ray events: the **non X-ray background**. Most of it is vetoed out by a cryogenic anti-coincidence detector located directly below the array and intercepting particles going through the matrix [2].

► ... the detector wafer inducing heat waves perturbing the pixels signal (similar to spikes observed in Planck HFI, [3]).

Expected distribution of energy depositions obtained with Geant4 simulations performed by INAF at Solar minimum (maximum CR flux, [4]).

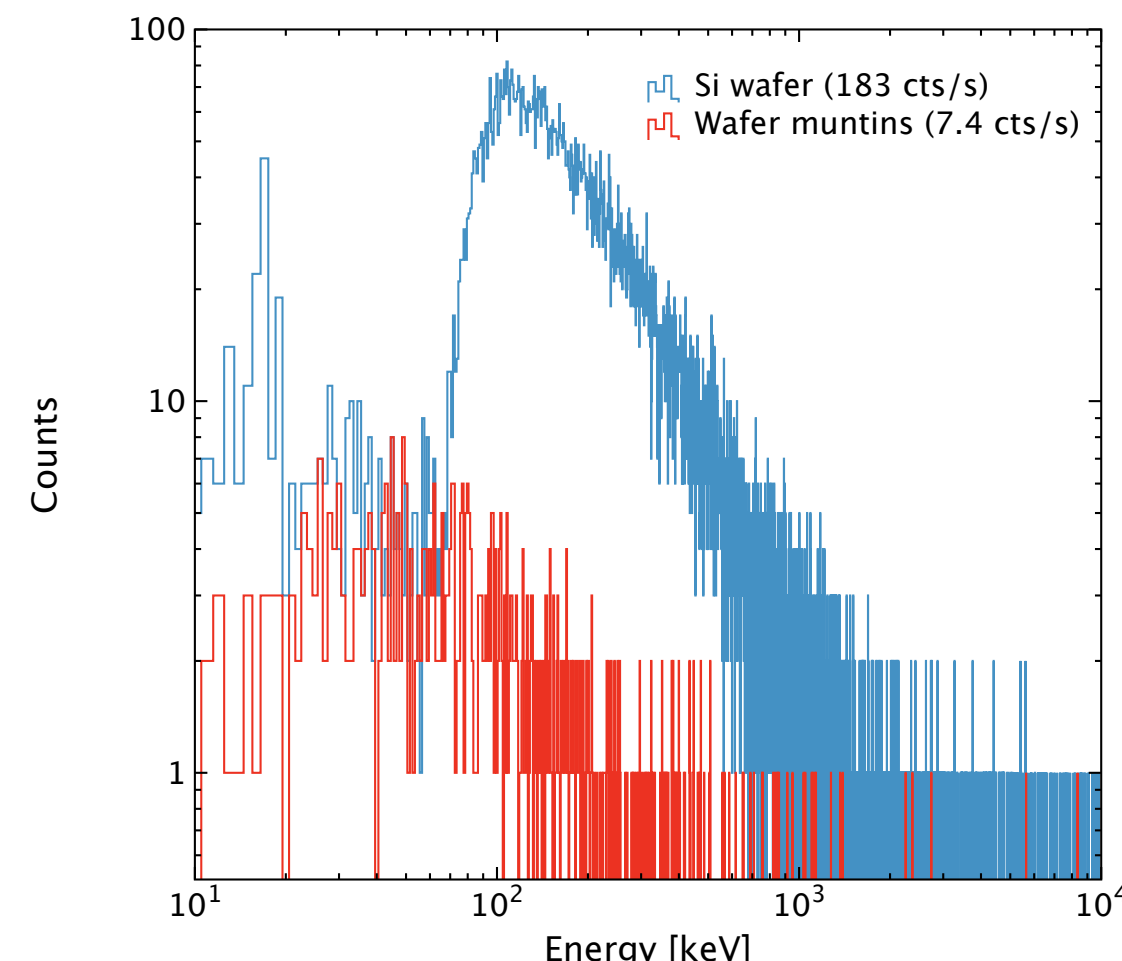


Figure 1: Left: Spectrum of CR induced energy depositions in the Si frame and muntin structure.

EFFECT ON ENERGY MEASUREMENT

Simulated the response of the TES detectors using the **xifusim** X-IFU readout chain simulator (see Poster 251 by M. Lorenz) by considering the wafer temperature oscillations as fluctuations of the pixels' thermal bath.

► The pixel response is purely thermal and therefore **much slower** than an X-ray electro-thermal response.

Studied the effect of CR events on the reconstructed energy of a 7 keV pulse as a function of their time separation (Fig. 7).

► Typical time window to get a significant energy influence is a **few ms** coincidence.

► Easily the case for frame events but quite rate for energy deposition in the muntin (only 7 cps).

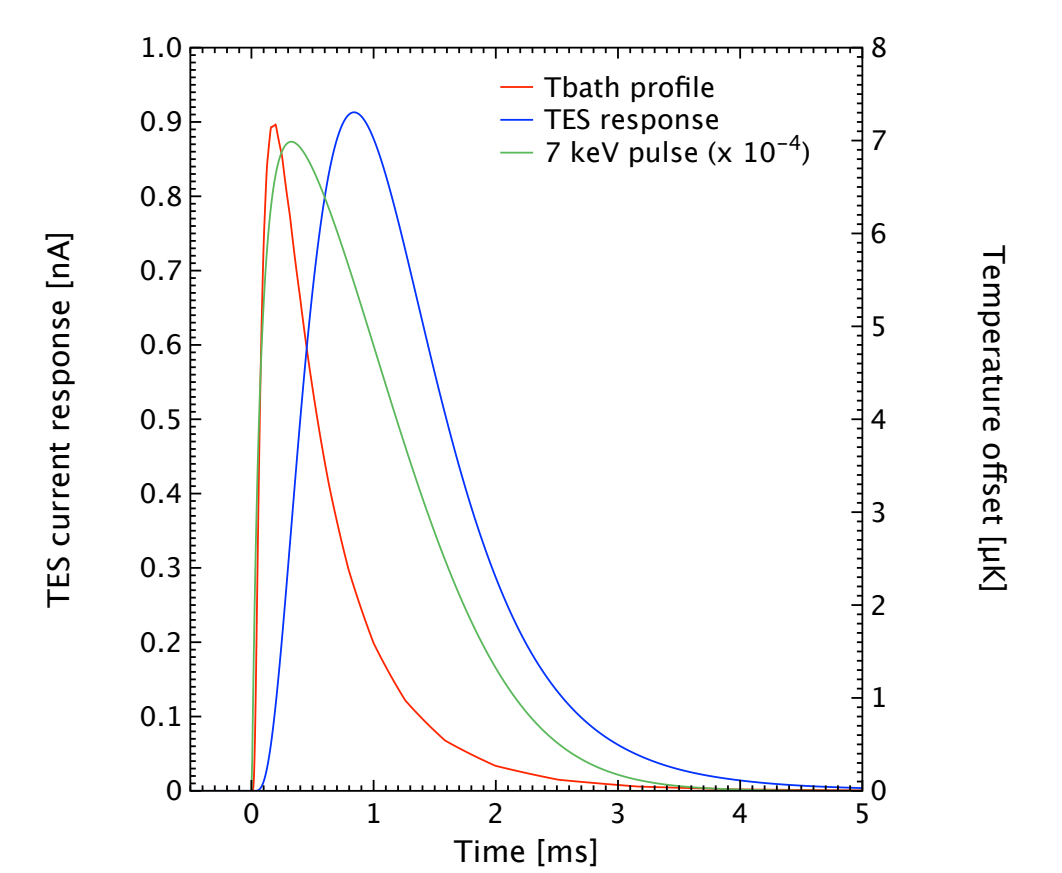


Figure 6: TES response to a thermal pulse compared to an X-ray pulse.

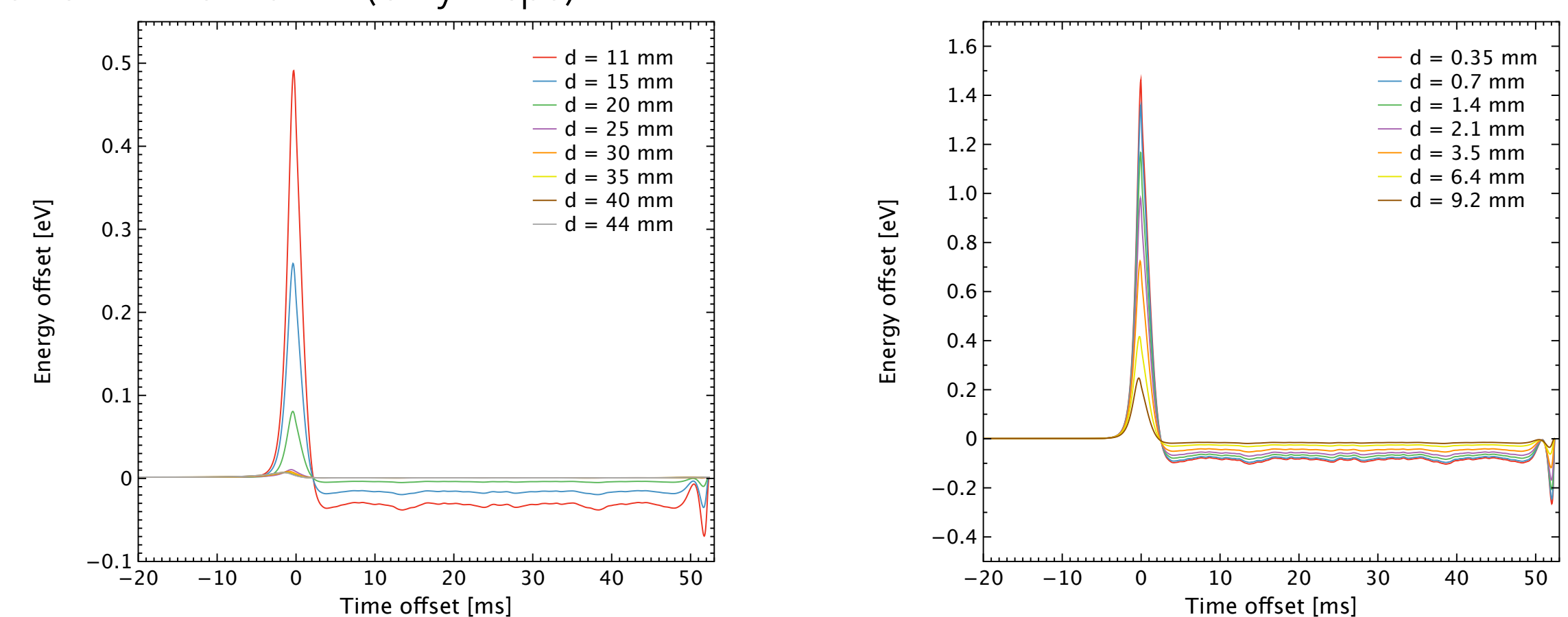


Figure 7: Energy offset measured on an 7 keV X-ray event recorded in the central pixel from a CR event at varying time offset and distance. All profiles are shown for the baseline heatsinking design and for the average energy deposition. Left: Frame hit (450 keV). Right: Muntin hit (255 keV).

To assess the average effect on the energy reconstruction, we simulated **10 000 random bath timelines** for each configuration and measured their effect on a 7 keV pulse reconstructed with optimal filtering (Fig. 8).

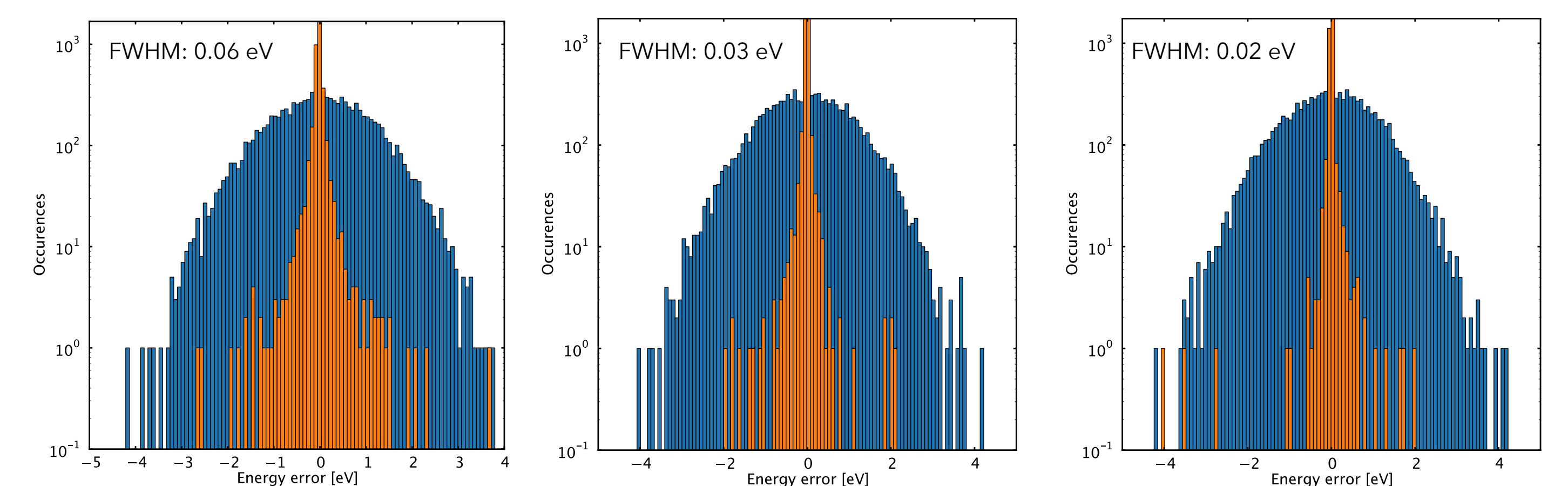


Figure 8: Histogram of the energy errors induced by cosmic ray hits in 3 simulation scenarios (orange). For comparison, a realization of the 2.5 eV FWHM instrument gaussian broadening is shown in blue. The quoted FWHM values were measured from the 88th and 12th percentiles of the distribution. Left: Frame hits for a side (worst case) pixel and the baseline heatsinking design. Middle: Same with the optimized design. Right: Muntin hits for the central pixel (worst case).

Inner broadening well within the 0.2 eV resolution degradation allocation
Larger offsets concern a small fraction (1.2%) of the events with the baseline design
The optimized heatsinking design reduces this fraction down to 0.5 %

TES WAFER THERMAL RESPONSE SIMULATIONS

The X-IFU will operate an array of more than 3000 **Transition Edge Sensor (TES)** microcalorimeters integrated in a Si frame. The TES themselves are deposited on a thin SiN membrane. The back of the array is etched up to the SiN membrane, forming a muntin structure. This structure is coated in gold to improve the array heatsinking to the cold bath.

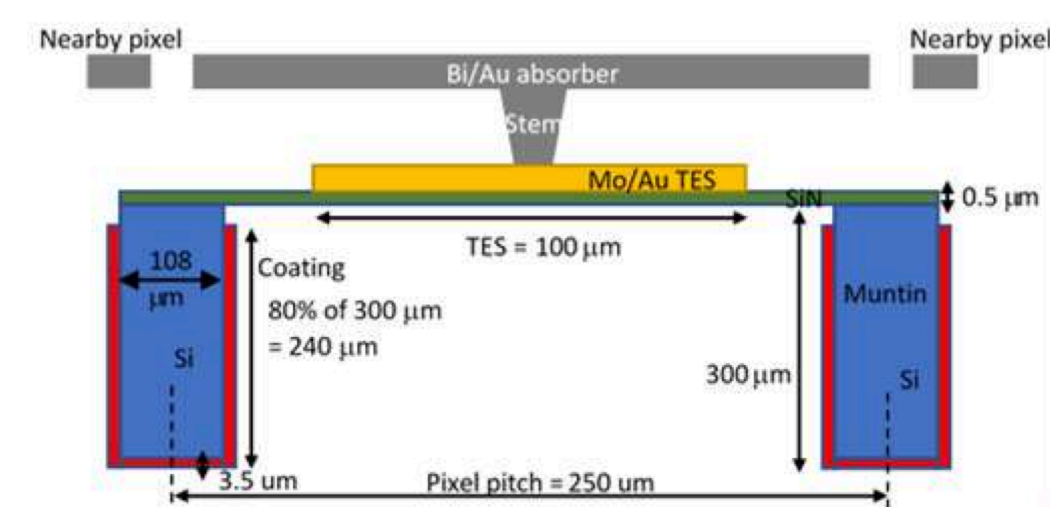


Figure 2: The TES array deposition structure.

The wafer **thermal response** was modeled and characterized by GSFC for two heatsinking configurations (see more details in Poster 128 by A. Miniussi) as a function of the CR impact position for a pixel at the center and at the edge of the array:

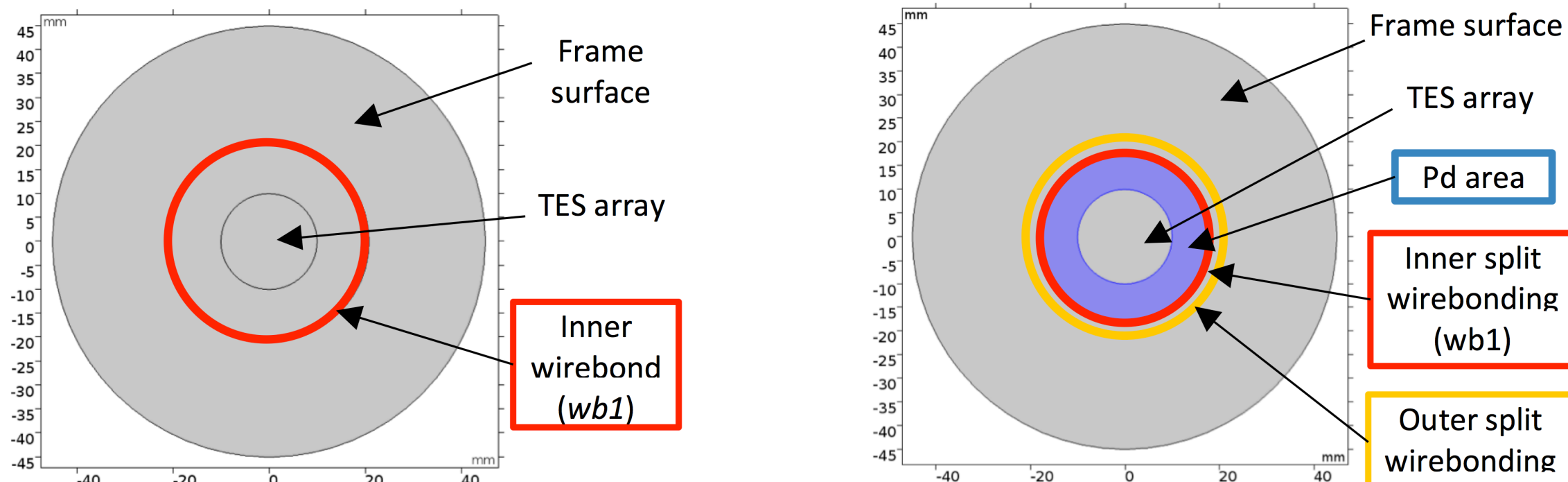


Figure 2: Simulated heatsinking geometries. Left: Baseline configuration with 1000 wirebonds at the wb1 location and a gold back coating of 3.5 μm thickness. Right: Optimized configuration with an additional Pd coating to damp the thermal response near the TES array and a split in the Au coating on the frame to limit the conductivity towards the periphery.

The **muntin structure** below the TES array (partially etched Si frame, see Fig. 2) was also simulated with a finely meshed model to handle the wafer response to energy depositions in the muntins.

► Shows **very large but short temperature pulses**

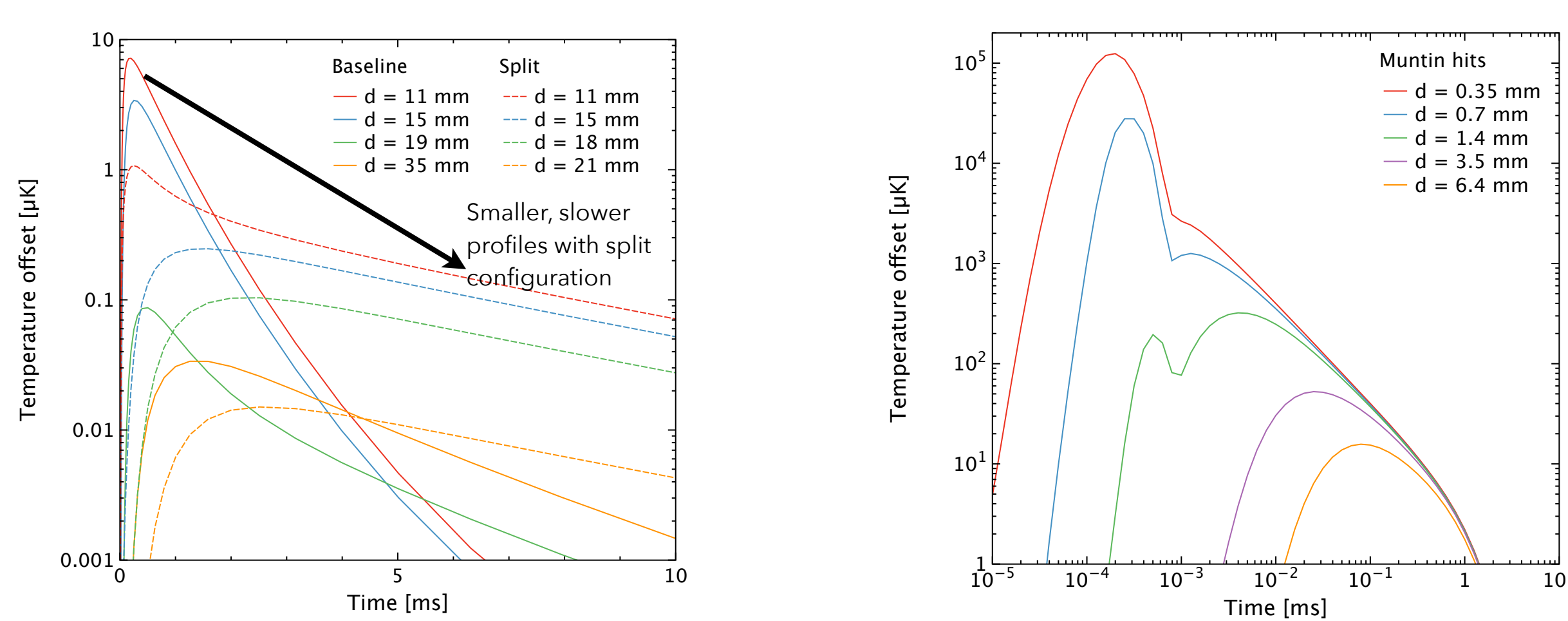


Figure 3: Simulated temperature pulses measured at the center of the array for CR impacts at varying distances (500 keV). Left: Impacts in the Si frame for both studied configurations. Right: Impacts in the muntin structure below the pixels.

THERMAL BATH TIMELINE SIMULATIONS

Created realistic **bath temperature timelines** by:

- Drawing a random CR arrival time from a Poisson distribution
- Drawing a random CR hit position assuming a flat distribution over the wafer
- Selecting a random energy deposition from the Geant4 event list
- Interpolating the induced temperature profile at the level of the victim pixel (see Fig. 4) and adding it to the timeline assuming linearity (verified in wafer thermal response simulations)

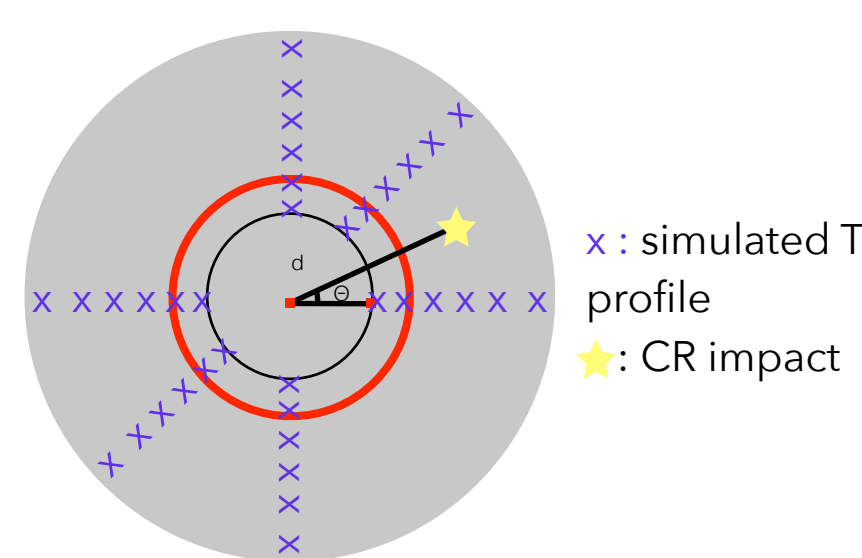


Figure 4: Schematics of the interpolation scheme.

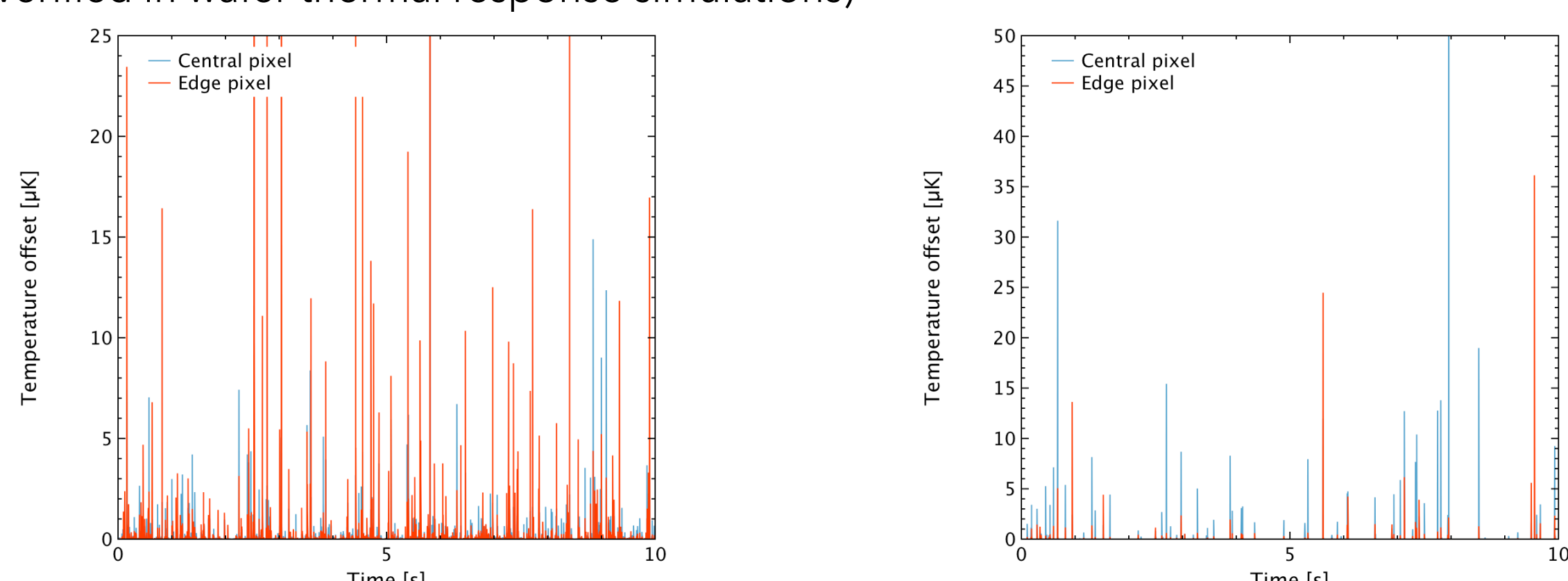


Figure 5: Example of bath temperature timelines for the baseline wafer configuration. Left: For CR hits in the Si frame. Right: For CR hits in the muntin structure.

Frame hits induce larger bath fluctuations for an edge than a central pixel
Muntin hits induce large but rare and short fluctuations

TRIGGERING CAPABILITY

Simulations show that **the standard X-ray trigger cannot detect these thermal events** as it is optimized to pick up much faster signals.

Studied with xifusim how a trigger on a decimated and low-pass filtered signal could more easily trigger cosmic ray events

► Optimum window found to be at ~1ms for the current best estimate pixel and noise level (Fig. 10).

► **Associated dead time computed to be << 1%.**

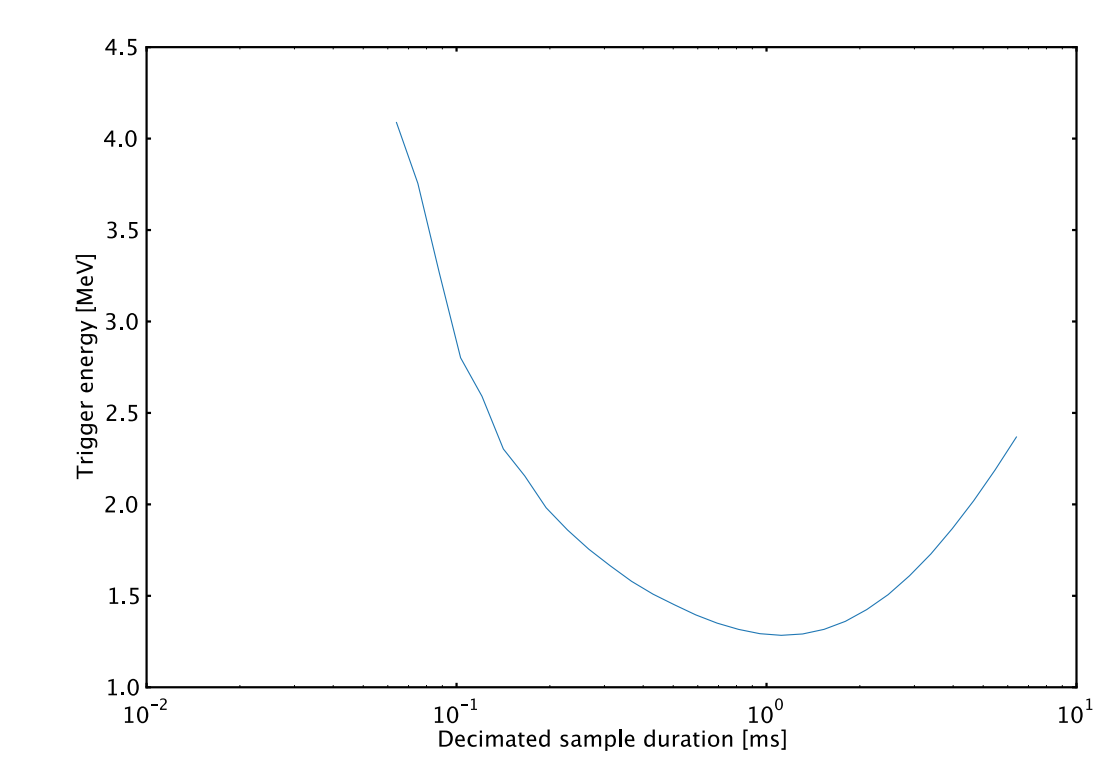


Figure 10: Optimization of the decimation factor for CR triggering.

Made a comparison between the energy at which the optimal trigger can detect the perturbation and the level at which such an event can create a certain energy offset (Fig. 11).

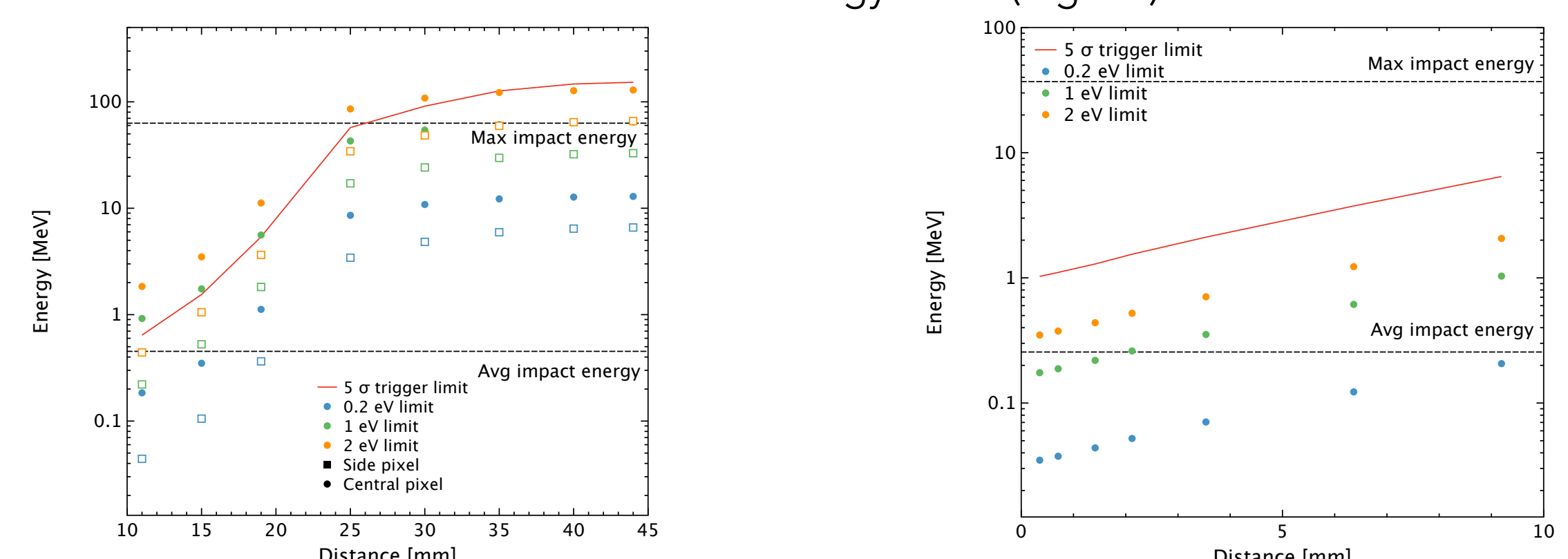


Figure 11: Comparison between trigger level and energy at which a CR deposition can induce different energy offsets. Left: For hits in the frame and the baseline heatsinking design. The trigger pixel is assumed to be on the edge of the array. Right: For hits in the muntin structure for a pixel and its trigger located at the center of the array.

A trigger on edge pixels could remove >1-2 eV offsets generated by frame hits
Relevant muntin hits cannot be triggered out

References:

- [1] Barret et al. 2018, Proceedings SPIE, Vol 10699, 106991G
- [2] D'Andrea et al. 2018, Proceedings SPIE, Vol 10699, 106994T
- [3] Planck collaboration 2013, A&A, Vol 571, A10
- [4] Lotti et al. 2018, Proceedings SPIE, Vol 10699, 106991Q